In Vivo Identification of Adducts from the New Hypoxia-Activated Prodrug CP-506 Using DNA Adductomics

Chemical Research in Toxicology

pubs.acs.org/crt

Article

In Vivo Identification of Adducts from the New Hypoxia-Activated Prodrug CP-506 Using DNA Adductomics

Morwena J. Solivio, Alessia Stornetta, Julie Gilissen, Peter W. Villalta, Sofie Deschoemaeker, Arne Heyerick, Ludwig Dubois, and Silvia Balbo*

Cite This: *Chem. Res. Toxicol.* 2022, 35, 275−282

Read Online

ACCESS | Metrics & More | Article Recommendations | Supporting Information

ABSTRACT: Many chemotherapeutic drugs exert their cytotoxicity through the formation of DNA modifications (adducts), which interfere with DNA replication, an overactive process in rapidly dividing cancer cells. Side effects from the therapy are common, however, because these drugs also affect rapidly dividing noncancerous cells. Hypoxia-activated prodrugs (HAPs) have been developed to reduce these side effects as they preferentially activate in hypoxic environments, a hallmark of solid tumors. CP-506 is a newly developed DNA-alkylating HAP designed to exert strong activity under hypoxia. The resulting CP-506-DNA adducts can be used to elucidate the cellular and molecular effects of CP-506 and its selectivity toward hypoxic conditions. In this study, we characterize the profile of adducts resulting from the reaction of CP-506 and its metabolites CP-506H and CP-506M with DNA. A total of 39 putative DNA adducts were detected in vitro using our high-resolution/accurate-mass (HRAM) liquid chromatography tandem mass spectrometry (LC−MS^3) adductomics approach. Validation of these results was achieved using a novel strategy involving ^{15}N-labeled DNA. A targeted MS/MS approach was then developed for the detection of the 39 DNA adducts in five cancer cell lines treated with CP-506 under normoxic and hypoxic conditions to evaluate the selectivity toward hypoxia. Out of the 39 DNA adducts initially identified, 15 were detected, with more adducts observed from the two reactive metabolites and in cancer cells treated under hypoxia. The presence of these adducts was then monitored in xenograft mouse models bearing MDA-MB-231, BT-474, or DMS114 tumors treated with CP-506, and a relative quantitation strategy was used to compare the adduct levels across samples. Eight adducts were detected in all xenograft models, and MDA-MB-231 showed the highest adduct levels. These results suggest that CP-506-DNA adducts can be used to better understand the mechanism of action and monitor the efficacy of CP-506 in vivo, as well as highlight a new role of DNA adductomics in supporting the clinical development of DNA-alkylating drugs.

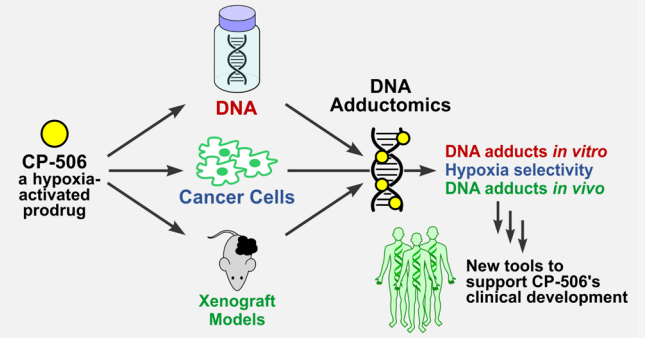

INTRODUCTION

Despite their approval as anticancer agents more than 60 years ago, DNA-alkylating drugs are still considered first-line medication for the treatment of a vast majority of cancers. Their mode of action involves covalent binding with DNA to form genotoxic modifications (adducts). These adducts can involve one base (monoadduct) or two bases on the same or opposite DNA strand (cross-linked adduct). In general, DNA cross-linked adducts are anticipated to be more toxic than monoadducts. Once formed and if not repaired, adducts interfere with DNA replication, which is overactive in rapidly dividing cancer cells.[1,2]

A drawback of chemotherapy with DNA-alkylating anticancer drugs is that due to their inability to selectively target cancer cells, they often cause unwanted side effects in treated patients.[2] Strategies pursued to reduce the side effects from these agents have resulted in the development of drugs that are preferentially activated in cellular environments found more prevalently in cancerous but not in noncancerous tissues. One example of such environment is hypoxia or anoxia, referring to a partial or total lack of oxygen, respectively. Following this concept, several hypoxia-activated prodrugs (HAPs) have been designed for oxygen-selective chemotherapy based on their ability to target the tumor hypoxic microenvironment. Ideally, HAPs are not toxic under normoxia (normal oxygen levels) because they do not result in toxic metabolites if oxygen is present.[3−8] Nitroaromatic-based HAPs have shown promising results, and among them, dinitrobenzamide mustard PR-104

Received: September 24, 2021
Published: January 20, 2022

https://doi.org/10.1021/acs.chemrestox.1c00329
Chem. Res. Toxicol. 2022, 35, 275−282

Scheme 1. Mechanism of the Metabolic Activation of CP-506

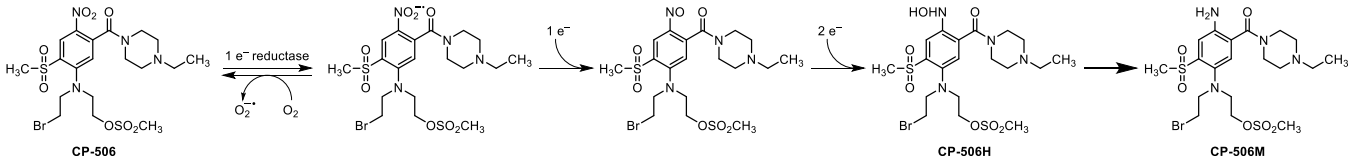

demonstrated selective hypoxic activation in a wide range of cancer cells and human tumor xenografts.[9]

PR-104 was initially tested in a number of clinical trials in combination with other antineoplastic drugs. However, patients experiencing severe dose-limiting myelotoxicity limited further testing.[10,11] Subsequent studies revealed that PR-104 can be activated by human two-electron aldo-keto reductase 1C3 (AKR1C3) independently from oxygen levels.[12] AKR1C3 is expressed in several healthy tissues, most notably in myeloid progenitor cells, likely explaining the observed myelotoxicity.[12]

We have previously developed a high-resolution/accurate-mass (HRAM) liquid chromatography tandem mass spectrometry (LC−MS^3) DNA adductomics approach to characterize the DNA damage originated from the reaction of the alcohol of PR-104, PR-104A, or its metabolites with DNA.[13] The approach uses data-dependent constant neutral loss (CNL) monitoring of either the deoxyribose moiety or any of the four DNA bases and triggers an MS^3 fragmentation of the resulting product ion, which confirms the presence of an adduct and can be used for structural elucidation.[13,14] This approach presents a more comprehensive way to perform DNA adductomics studies since it allows us to also screen for nucleobase adducts and its application allowed for the characterization of both mono- and cross-linked adducts induced by PR-104A and its metabolites.[13] This approach was also applied to gain further insights into the selectivity of PR-104A toward hypoxia and cancer cells.[15,16]

Recently, a next-generation HAP called CP-506 (Scheme 1) was developed and is currently being prepared for clinical evaluation. CP-506 was designed to overcome a number of limitations of PR-104, such as improved solubility, no reduction by AKR1C3, and activation only under severely low oxygen levels.[17] In hypoxic environments, CP-506 is initially reduced to a short-lived intermediate and then further reduced to active hydroxylamine (CP-506H) and amine (CP-506M) metabolites (Scheme 1). These metabolites then exert their cytotoxic effects by reacting with DNA.[17]

To further increase our understanding about the nature of the DNA adducts and the selectivity toward hypoxia of CP-506, the goal of this study was to characterize the DNA adducts induced by CP-506, CP-506H, and CP-506M first in purified DNA exposed to the drug or its metabolites, then in cancer cells exposed to CP-506 under anoxic or normoxic conditions, and finally in vivo in three tumor xenograft models. A total of 39 adducts were identified in vitro, and eight of them were subsequently detected in vivo. These results demonstrate the ability of our methodology to measure adducts to monitor CP-506's efficacy in complex biological samples, with potential use in assessing patient susceptibility and side effects in the upcoming clinical trials using CP-506.

■ EXPERIMENTAL PROCEDURES

Full details regarding the generation of ^{15}N-labeled DNA, cell cultures of cancer cell lines, DNA isolation from cells and xenograft models, and quantitation of DNA can be found in the Supporting Information. Calf thymus DNA (ctDNA) was purchased from Worthington Biochemical Corporation (Lakewood, NJ). CP-506 {2-[(2-bromoethyl)-5-[(4-ethyl-1-piperazinyl)carbonyl]-2-(methylsulfonyl)-4-nitroanilino]ethyl methanesulfonate}, CP-506H [2-((2-bromoethyl)(5-(4-ethylpiperazine-1-carbonyl)-4-(hydroxyamino)-2-(methylsulfonyl)phenyl)amino)ethyl methanesulfonate], and CP-506M [2-((4-amino-5-(4-ethylpiperazine1-carbonyl)-2-(methylsulfonyl)phenyl)(2-bromoethyl)amino)ethyl methanesulfonate] were manufactured by Mercachem employing synthetic routes developed at the University of Auckland.[17]

Unless specified, all other reagents, solutions, and enzymes were obtained from Qiagen and Sigma-Aldrich.

Treatment of ctDNA and ^{14}N- or ^{15}N-Labeled Bacterial DNA with CP-506, CP-506M, or CP-506H. A 10 μL volume of 10 mM CP-506, CP-506M, or CP-506H in dimethyl sulfoxide (DMSO) (Tocris Bioscience; Minneapolis, MN) was added to 990 μL of a 1 mg/mL solution of DNA in 10 mM Tris-HCl, 1 mM ethylenediaminetetraacetate (pH 7.4) to a final drug or metabolite concentration of 100 μM, and 0.01% DMSO. The same volume of DMSO was added to a negative control sample containing the same concentration of DNA. The samples were incubated at 37 °C overnight (~16 h).

DNA Cleanup. A 1 mL volume of cold 100% isopropanol (Honeywell; Charlotte, NC) was added to the reaction mixtures to precipitate the DNA. The tubes were inverted 20 times, placed on ice for 10 s, and inverted again to ensure DNA precipitation. The tubes were then centrifuged at 1000*g* (Beckman Coulter Allegra-X-3OR; Brea, CA) for 2 min. The DNA pellet settled at the bottom of the tubes, and the supernatant was poured out. Sample purification was accomplished by adding 4 mL of a cold 70% isopropanol solution to the tubes and by vortexing for 1 min before centrifugation for 2 min at 1000*g*. The supernatant was subsequently discarded. The cleanup process was repeated four more times to ensure that any excess of the prodrug or its metabolites was eliminated. Finally, 4 mL of cold 100% isopropanol was added into each tube, and the tubes were shaken gently and then centrifuged at 2000*g* for 5 min. The supernatant was discarded, and the tubes were inverted on clean, absorbent paper towels and left to dry for 15 min. The samples were then resuspended in 900 μL of 10 mM Tris-HCl and 5 mM $MgCl_2$, pH 7.4. The DNA concentrations were determined using a nanodrop spectrophotometer (Eppendorf Biophotometer; Hauppauge, NY).

Xenograft Tumor Tissue Treatment. Tumors were initiated in 10−11 week old female NCr nude mice with body weights ranging from 20 to 28 g by subcutaneous implantation of 5×10^6 cells in phosphate-buffered saline (PBS) (0.1 mL suspension) into the right flank of each animal; DMS11: 5×10^6 cells in 50% PBS−Matrigel matrix (BD Biosciences) injected into the right flank of female NCr [Crl:Nu(NCr)-*Foxn1*^{nu}] mice, 10−11 weeks old and 20.2−28 g weight, or 1×10^7 cells in PBS (0.1 mL) in the right mammary fat pad; BT-474: 1×10^7 cells in 50% PBS−Matrigel matrix (Corning) injected into the right flank of female NOD/SCID mice, 6−7 weeks old and 16.2−21.8 g weight; and MDA-MB-231: 1×10^7 cells in 50% PBS−Matrigel matrix (Corning) injected into the right flank of female Balb/c nude mice, 6−7 weeks old and 17.2−21.4 g weight. When the tumors reached the target volume of 225−250 mm^3, the mice were sorted into two groups. The control group received the vehicle (2% DMSO and 0.85% NaCl in water), while the second group received 600 mg/kg body weight CP-506 administered intraperitoneally (i.p.) Mice received either the vehicle or CP-506 once daily for 2 days. Sampling/euthanasia was conducted 24 h after the last treatment for

https://doi.org/10.1021/acs.chemrestox.1c00329
Chem. Res. Toxicol. 2022, 35, 275−282

BT474 and MDA-231 and 5 h after the last treatment for DMS114. Tumor samples were collected, snap-frozen, and stored at −80 °C until further processing.

Enzyme Hydrolysis and Removal. Enzyme hydrolysis was initiated by adding 120 units (U)/mg DNA of DNAse I, followed by overnight (~16 h) shaking in a 37 °C water bath. The following day, another 120 U/mg DNA DNAse I was added, along with 4 mU/mg DNA of phosphodiesterase I and 48 U/mg DNA of alkaline phosphatase (Roche; Indianapolis, IN). Enzymes were then removed using Amicon Ultra-0.5 centrifugal filter devices with a 10,000 nominal molecular weight limit according to the manufacturer's instructions. A 10 μL aliquot was removed from each sample and transferred into 1.2 mL silanized vials (Chromtech; Apple Valley MN) for the quantitation of dG by high-performance LC (HPLC).

Sample Enrichment. Solid phase extraction (SPE) was conducted on the hydrolyzed samples using a 33 μm reverse-phase Strata-X cartridge (Phenomenex; Torrance, CA). The cartridge was activated by three 1 mL volumes of 100% methanol (Honeywell; Charlotte, NC) and equilibrated by 1 mL of LC−MS-grade water (Fisher Scientific; Hampton, NH) before the loading of the samples. The cartridges were then washed with three 1 mL volumes of LC−MS-grade water and then with 1 mL of 10% methanol, and a 1 mL volume of 100% methanol was collected. Collected fractions were dried using a Savant SC210A SpeedVac concentrator (Fisher Scientific; Waltham, MA) prior to LC−MS analysis.

Sample Resuspension for MS. CtDNA-/bacterial DNA-treated and negative control samples were prepared in duplicate. One replicate was resuspended in 100 μL of 20% methanol, whereas the other one was resuspended in 500 μL of 20% methanol, which was accomplished by adding methanol, followed by sonication for 5 min, addition of LC−MS-grade water, and another 5 min sonication. Cell and tissue DNA samples were resuspended in 20 and 50 μL of 20% methanol, respectively.

LC−CNL−MS^n Data-Dependent Acquisition in ctDNA and Bacterial DNA Samples. All LC−MS experiments were performed on an Orbitrap Fusion mass spectrometer (Thermo Scientific, Waltham, MA) coupled to a Dionex RSLCnano ultra-performance liquid chromatograph (Thermo Scientific, Sunnyvale, CA). Reverse-phase chromatography was performed with a hand-packed Luna C18 column (5 μm, 120 Å, 200 mm × 75 μm ID, Phenomenex, Torrance, CA) at room temperature and a flow rate of 0.3 μL min^{-1} using 5 mM ammonium acetate as mobile phase A and acetonitrile as mobile phase B. The LC gradient started at 5% B for the first 5 min with a flow rate of 1.0 μL min^{-1}, followed by the switching of the injection valve to remove the 5 μL loop from the flow path and reducing the flow rate to 0.3 μL min^{-1} over 1 min. A linear gradient from 5 to 45% B over 39 min was used, which was then ramped to 98% B over 1 min. The mobile phase composition was allowed to stay at 98% B for 4 min. Finally, re-equilibration was performed by changing the mobile phase composition from 95 to 5% B over 1 min, increasing the flow rate to 1.0 μL min^{-1} over 1 min, and then holding at 5% B for 3 min. The total run time was 55 min.

CNL−MS^n data-dependent acquisition (DDA) was performed with the instrument operating in the positive ionization mode by repeated full-scan detection, followed by MS^2 acquisition and CNL triggering of MS^3 fragmentation over a cycle time of 2 s. Full-scan (range 300−2000 Da) detection was performed by setting the Orbitrap detector at 60,000 resolution, using EASY-IC internal mass calibration, automatic gain control (AGC) target settings of 2.0 × 10^5, and the maximum ion injection time set to be 50 ms. The MS^2 fragmentation parameters were as follows: a quadrupole isolation window of 1.6 amu, a higher energy collisional dissociation (HCD) stepped collision energy of 20% ± 10%, Orbitrap detection at a resolution of 15,000, an AGC of 5.0 × 10^4, and a maximum injection time of 22 ms. Data-dependent conditions were as follows: a triggering intensity threshold of 2.5 × 10^4, a repeat count of 1, and an exclusion duration of 30 s.

The MS^3 fragmentation parameters were as follows: 2 amu isolation window, an HCD stepped collision energy of 20% ± 10%, Orbitrap detection at a resolution of 7500, an AGC of 2.0 × 10^5, and a maximum injection time of 50 ms. Fragmentation was triggered upon the observation of the neutral loss of dR (−116.0474), adenine (−135.0545)/^{15}N-adenine (−140.0397), guanine (−151.0494)/^{15}N-guanine (−156.0346), cytosine (−111.0433)/^{15}N-cytosine (−114.0344), or thymine (−126.0429)/^{15}N-thymine (−128.03688) between the parent ion from the full scan (untargeted adductomics) and one of the product ions or between the parent ion from the full scan that was also present in a list of 108 predicted CP-506, CP-506M, or CP-506H adducts and cross-link masses (targeted adductomics) and one of the product ions, provided a minimum signal of 2.5 × 10^4. The threshold for mass accuracy was set at 5 ppm for all masses.

A total of about 6 μg of ctDNA and 6 and 15 μg of a 1:1 mixture of ^{14}N- and ^{15}N-labeled hydrolyzed and purified bacterial DNA, respectively, were injected for analysis using the untargeted adductomics approach.

Targeted MS/MS Analysis of Cancer Cell Lines In Vitro and Tumor Xenografts In Vivo. For the cancer cell samples, 5−10 μg of DNA was processed and purified prior to LC−MS analysis, whereas for the xenograft tumor tissue DNA, between 43 and 550 μg of DNA was processed, purified, and spiked with a mixture of ^{15}N-labeled DNA adducts. Chromatography conditions were the same as the one used for the analysis of in vitro samples. Targeted MS/MS was performed with the following parameters: Orbitrap detection at a resolution of 60,000, an HCD stepped collision energy of 30 ± 10%, a quadrupole isolation window of 1.6 amu, an AGC of 5.0 × 10^4, a maximum injection time of 118 ms, and a mass range of 100−850. The threshold for mass accuracy was set at 5 ppm for all masses. All masses reported in Figure 3 were targeted in the cell line and tumor xenograft DNA samples.

RESULTS

The goal of this work was to characterize the DNA adducts resulting from the newly developed HAP CP-506 and its cytotoxic metabolites CP-506H and CP-506M (Scheme 1) in vitro and to verify their presence in vivo. The presence of the identified DNA adducts was then tested in a panel of five cancer cell lines, and their relation to hypoxic conditions was investigated. We initially exposed ctDNA and isotope-labeled bacterial DNA to CP-506 or its metabolites. Exposed and unexposed DNA samples were enzymatically hydrolyzed, and the resulting adducts were separated from the unreacted nucleosides and enriched. DNA adduct screening was performed using our untargeted DNA adductomics approach, which is based on MS^3 fragmentation upon observation in MS^2 spectra of the exact mass neutral loss of either the deoxyribose moiety or any of the four DNA bases.[13,14]

The data analysis workflow for the in vitro work is shown in Figure 1. The masses that triggered MS^3 events in the drug treatment and control samples are compared, and extracted ion chromatograms (EICs) are created for those unique (within ±5 ppm) to the treated samples. The EICs are visually examined to confirm the absence of a signal in the negative control and a reasonable chromatographic peak in the treated sample with MS^2 and MS^3 events at the appropriate retention times (see also Figure 2). The MS^2 and MS^3 fragmentation spectra are then used to predict the structure of the putative DNA adducts, and the parent masses are used to calculate the molecular formulas. The resulting structures are then compared to adduct structures for the drug analogue to CP-506, assuming that the information is available.

Finally, the presence of the resulting adducts is further confirmed using ^{14}N- and ^{15}N-DNA exposed to the drug or metabolites, processed as described above, and mixed in a 1:1 ratio prior to LC−MS analysis (Figure S1). In this resulting sample, the presence of coeluting peaks and MS^3 events corresponding to ^{14}N- and ^{15}N-labeled versions of the same

https://doi.org/10.1021/acs.chemrestox.1c00329
Chem. Res. Toxicol. 2022, 35, 275−282

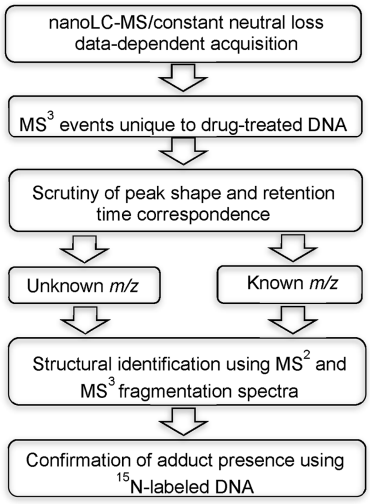

Figure 1. Data analysis flowchart for the identification and confirmation of DNA adducts.

adduct substantiates adduct identification. A representative example of this confirmation analysis is shown in Figure 2. The data reported here refer to a cross-linked DNA adduct resulting from the alkylation of CP-506 and two guanine bases. In this example, the alkylating portion (calculated, m/z 409.1541) is derived from the difference between the parent ion (calculated, m/z 711.2529) and the mass corresponding to the neutral loss of the two guanine bases (calculated, 302.0988).

Thirty-nine putative DNA adducts resulting from CP-506, CP-506H, or CP-506M were found in ctDNA and ^{14}N-/^{15}N-labeled DNA, as detected by the neutral loss of dR, A, G, or C (Table 1). These masses included both monoadducts and cross-links (seven out of the total). Out of the seven cross-linked adducts, three resulted from CP-506, whereas four resulted from amine metabolite CP-506M. CP-506M formed the most adducts with 21 adducts detected, followed by CP-506 with 14, and the hydroxylamine metabolite CP-506H with 4 (Table 1).

The detection of 14 adducts in the CP-506-treated sample indicates that at the tested concentrations, the prodrug itself alkylates DNA. Two of these adducts matched the predicted structures from the alkylation of the two CP-506 metabolites and DNA (numbers 5 and 16 in Table 1). We hypothesized that their formation is due to some metabolite impurities not removed during the chemical synthesis of CP-506. This hypothesis was tested by the analysis of a solution of CP-506 by LC−MS, which showed the presence of the two metabolites and other degradation products (data not shown). However, it cannot be excluded that the metabolites are byproducts from the incubation using in vitro experimental conditions.

In the CP-506H- and CP-506M-treated samples, an interesting finding was the observation of m/z 666.3028 (adduct numbers 29 and 30 in Table 1), detected by the neutral loss of dR in both samples. This mass matches the structure of either a monoadduct between dG and CP-506M or a monoadduct between dA and CP-506H. The MS^2 spectrum resulting from the analysis of the CP-506H-treated sample shows fragments corresponding to both guanine and adenine (Figure S2), indicating that both adducts are present in the sample and suggesting that the metabolites used in this experiment may also contain some impurities that were not removed during the chemical synthesis or that the conditions of our experiments resulted in the formation of byproducts. Further investigation of the origin of these adducts with purified metabolites or corresponding labeled versions will allow us to better characterize the nature of these modifications.

All 39 adducts detected in purified DNA were then targeted using MS/MS in five CP-506-exposed cancer cell lines: two pancreas, two breast, and one lung cell lines (Table S1). Each cell line was exposed to 100 μM CP-506 for 4 h under anoxic or normoxic conditions. The half maximal inhibitory

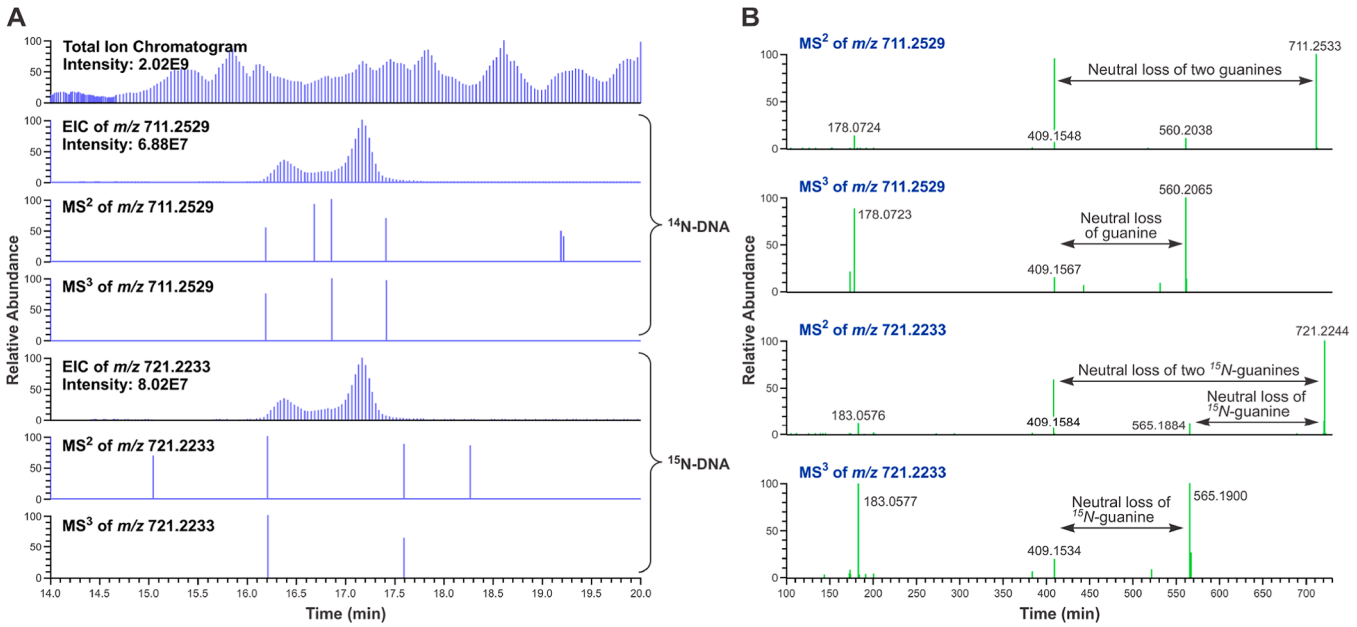

Figure 2. Representative example of DNA adduct detection and confirmation for a guanine−guanine cross-link. (A) Chromatograms for the ^{14}N- and ^{15}N-labeled versions of the adduct; (B) MS^2 and MS^3 spectra for the adduct containing either of the two nitrogen isotopes.

https://doi.org/10.1021/acs.chemrestox.1c00329
Chem. Res. Toxicol. 2022, 35, 275−282

Table 1. DNA Adducts from CP-506, CP-506H, and CP-506M Detected in Purified DNA Using Untargeted Adductomics and in Cancer Cell Lines Using Targeted MS/MS (the Latter Are Highlighted in Blue)[a]

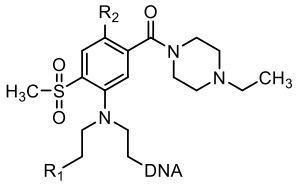

No.	Parent	Product	Neutral Loss	Adduct Type	Proposed R1	Proposed R2	CP-506		CP-506M		CP-506H		MDA-MB-468[b]		BT-474[b]		NCI-H1650[b]		SW1990[b]		Mia-Paca-2[b]	
							CtDNA	$^{14}N/^{15}N$-DNA Coupling	CtDNA	$^{14}N/^{15}N$-DNA Coupling	CtDNA	$^{14}N/^{15}N$-DNA Coupling	ANX	NRX	ANX	NRX	ANX	NRX	ANX	NRX	ANX	NRX
1	508.2336	397.1903	C	Base monoadduct	OH	NH2			X	X												
2	530.2293	379.1799	G	Base half mustard adduct	–	NH2			X	X			X				X		X		X	
3	532.2449	397.1904	A	Base monoadduct	OH	NH2			X	X	X	X			X		X		X		X	
4	546.2242	395.1747	G		OH	NH2			X	X	X	X	X		X		X		X		X	
5	548.2398	397.1904	G		OH	NH2	X	X	X	X	X	X	X		X	X	X		X		X	
6	550.2110	415.1565	A		Cl	NH2			X	X	X	X			X				X		X	
7	562.2191	411.1697	G	Base half mustard adduct	–	NO2		X			X	X										
8	562.2191	427.1646	A	Base monoadduct	OH	NO2	X	X			X	X										
9	564.2347	413.1853	G		OH	NHOH			X	X					X							
10	566.2059	415.1565	G		Cl	NH2			X	X			X		X		X		X		X	
11	566.2059	431.1514	A		Cl	NHOH					X											
12	578.2140	427.1646	G		OH	NO2	X	X			X	X										
13	580.1852	445.1307	A		Cl	NO2	X	X			X	X										
14	594.1605	459.1060	A		Br	NH2					X		X		X							
15	596.1801	445.1307	G		Cl	NO2	X	X			X	X										
16	610.1554	459.1060	G		Br	NH2	X				X	X										
17	610.2224	475.1679	A		OSO_2CH_3	NH2					X											
18	624.1347	489.0802	A		Br	NO2	X	X			X	X										
19	624.2810	508.2339	dR	Nucleoside monoadduct	OH	NH2			X	X												
20	640.1296	489.0802	G	Base monoadduct	Br	NO2	X	X	X	X	X	X	X	X	X	X	X	X	X	X	X	X
21	540.1966	505.1421	A		OSO_2CH_3	NO2		X			X	X										
22	642.2471	526.1997	dR	Nucleoside monoadduct	Cl	NH2				X												
23	648.2922	532.2448	dR		OH	NH2			X	X			X	X	X							
24	656.1915	505.1421	G	Base monoadduct	OSO_2CH_3	NO2	X	X	X		X	X	X	X	X	X	X	X	X	X	X	X
25	664.2871	548.2398	dR	Nucleoside monoadduct	OH	NH2			X	X			X		X						X	
26	665.2825	530.2291	A	Base crosslinked adduct	–	NH2					X	X										
27	665.2837	514.2343	G		–	NH2			X	X	X											
28	666.2583	550.2109	dR	Nucleoside monoadduct	Cl	NHOH				X	X	X	X		X			X	X			
29	666.3028	550.2554	dR		OH	NH2				X	X	X										
30	666.3028	550.2554	dR		OH	NHOH				X	X	X										
31	668.2740	552.2266	dR		Cl	NH2				X												
32	680.2821	564.2347	dR		OH	NO2						^{14}N-DNA ONLY										
33	681.2787	530.2293	G	Base crosslinked adduct	–	NH2			X	X	X	X	X		X		X					
34	695.2579	544.2085	G		–	NO2					X											
35	695.2579	560.2034	A		–	NO2	X	X			X											
36	711.2528	560.2034	G		–	NO2	X	X			X	X										
37	712.2235	596.1761	dR	Nucleoside monoadduct	Cl	NO2		X	X													
38	728.2854	612.2380	dR		OSO_2CH_3	NH2				^{14}N-DNA ONLY												
39	797.3260	681.2786	dR	Nucleoside crosslinked adduct	–	NH2			X	X	X	X	X		X						X	
						Total	11	13	17	21	27	22	12	3	14	3	8	3	9	2	10	2

[a]The structure proposed for each accurate mass detected is only a putative adduct attributed in light of the corresponding chemical formula. Absolute structural confirmation will only be possible by comparing the adducts with a synthetic standard. Abbreviations: dR, 2′-deoxyribose; G, guanine; A, adenine; C, cytosine; ANX, anoxic; and NRX, normoxic. [b]These data were also mentioned in the submitted report of van der Wiel et al.[17]

concentration (IC_{50}) values of CP-506 for each cell line under these conditions are reported in Table S1. Of the 39 adducts detected previously, 15 were also detected in one or more cancer cell lines (Table 1). When comparing the treatment conditions, we observed more adducts in cells treated under anoxia than those under normoxia (8−14 vs 2−3 adducts, depending on the cell line), indicating that the drug is preferentially activated to the reactive metabolites under hypoxic conditions. In addition, the more cytotoxic cross-linked adducts were detected only under hypoxic conditions. Thirteen out of the 15 adducts detected in cells resulted from CP-506M. The remaining two detected adducts resulted from the alkylation of guanine by CP-506. These two adducts were present in all cell lines and in both treatment conditions, which is not surprising considering that CP-506 adducts were detected in purified DNA as well and that CP-506's presence does not depend on oxygen levels. However, CP-506's reactivity toward DNA seems to be solely exerted toward the most reactive nucleophilic base guanine (Table 1).

The presence of CP-506-derived adducts was further investigated in vivo, in xenograft mouse models of MDA-MB-231 and BT-474, and in the small cell lung cancer xenograft DMS114. CP-506 (600 mg/kg of the body weight) or the vehicle (2% DMSO, 0.85% NaCl) was administered when the tumor reached an average volume of 250 mm^3 for two consecutive days. DNA extracted from these samples was processed and subjected to MS/MS, targeting the 39 adduct masses previously detected in vitro. To compare the adduct levels in the three models, DNA samples were spiked with an internal standard mixture consisting of a 1:1:1 ratio of ^{15}N-labeled CP-506, ^{15}N-labeled CP506H, and ^{15}N-labeled CP-506M adducts, all generated from the in vitro exposures, similarly to a strategy developed for the comparison of PR-104A-derived adducts.[15] The spiked concentration was adjusted to obtain the peak areas that were similar to those detected in the xenograft samples.

A total of eight DNA adducts were detected in MDA-MB-231-, BT-474-, and DMS114-bearing xenografts (Figure 3). BT-474 had the lowest level of each adduct, whereas MDA-MB-231 had the highest levels for most of the adducts and comparable levels to those of DMS-114 for some of the adducts (Figure 3). Five out of the eight adducts detected matched structures that contain the nitro group, indicating that these adducts most likely result from CP-506. One of these adducts was a G−G cross-link. The remaining three adducts resulted from amine metabolite CP-506M, and one of them was also a G−G cross-link (Figure 3).

https://doi.org/10.1021/acs.chemrestox.1c00329
Chem. Res. Toxicol. 2022, 35, 275−282

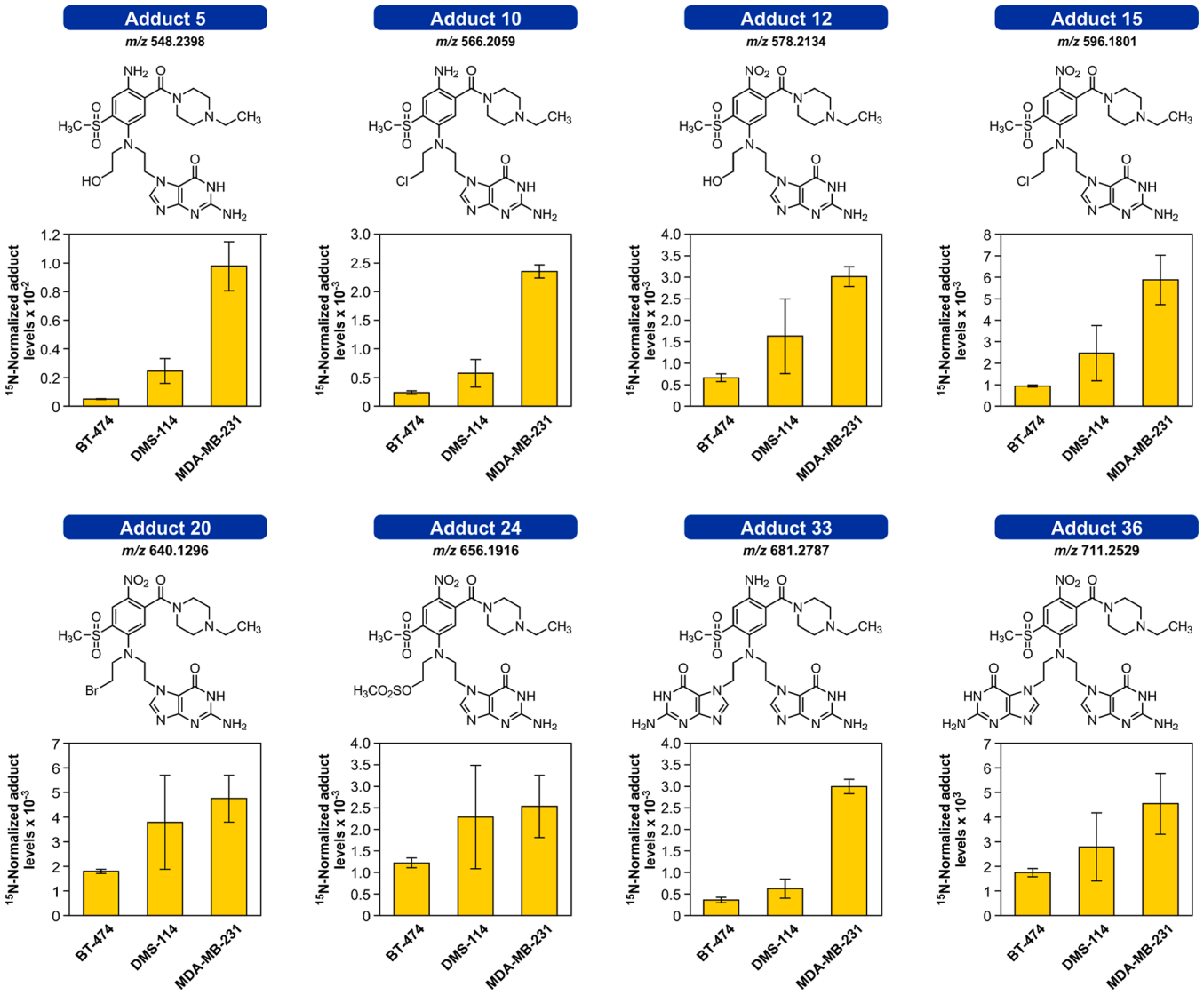

Figure 3. Relative levels of DNA adducts detected in xenograft models and structures of the corresponding proposed putative adducts. Structures are predictions based on the fragment observed and the structure of the drug; however, confirmation of the identity will only be possible by comparison with synthetic standards.

DISCUSSION

The use of biomarkers in drug discovery and early-stage testing is essential to shorten the development times, reduce costs by avoiding unnecessary studies, and increase the chances of success.[8,18] Biomarkers provide measurable endpoints to monitor the drug's mode of action and support dose escalation and patient stratification. In the case of the development of DNA-alkylating anticancer drugs, the modifications (adducts) resulting from the action of these drugs or their metabolites with DNA can be used to better characterize the mode of action, toxicities in different models, and the variables and conditions affecting the efficacy early on in the developmental process. Additionally, because DNA is the ultimate target of the drug, DNA adducts may be more suited (in contrast, e.g., to measure the drug's metabolites) to monitoring the effects in humans and supporting the execution of clinical trials.[19]

In this study, we characterized the DNA adducts induced by the experimental anticancer HAP CP-506 and its reactive hydroxylamine (CP-506H) and amine (CP-506M) metabolites. The main findings of this study were (a) a list of 39 DNA adducts detected in vitro in purified DNA; (b) information regarding the hypoxia selectivity of CP-506; and (c) detection and relative amounts of CP-506 adducts in vivo in three xenograft models. The reported adducts and methodologies can be used to monitor the drug efficacy and toxicity in future clinical studies of CP-506.

CP-506 was developed from PR-104 to overcome some limitations related to solubility and hypoxia selective activation.[17] Our in vitro data suggest that the structural changes performed on CP-506 improved the drug selectivity toward hypoxic conditions, as shown by more adducts being detected in anoxic versus normoxic treatment, but did not completely eliminate its ability to react directly with DNA. Table 1 summarizes the accurate masses of the adduct detected and the putative structures attributed as consistent with the corresponding chemical formula since absolute characterization will only be possible by comparison with synthetic standards. It is important to notice that CP-506 more readily alkylates to form monoadducts, whereas its metabolites more readily form the more cytotoxic cross-linked adducts under

https://doi.org/10.1021/acs.chemrestox.1c00329
Chem. Res. Toxicol. 2022, 35, 275−282

hypoxia. Whether this degree of selectivity is related to the treatment success without too many side effects needs further investigation. Nevertheless, our study provides a panel comprising 39 adducts from CP-506 and its metabolites to be monitored to answer this question in the future.

We were able to detect and monitor the levels of eight of the previously identified adducts in xenograft tumor tissue models bearing two of the cell lines previously tested (MDA-MB-231 and BT-474) and DMS114 (Figure 3). Similar to what was observed in vitro, CP-506 induced adducts in vivo without being first reduced to the two metabolites (five adducts were indeed from CP-506, whereas the other three adducts resulted from CP-506M). These findings could derive from the lower selectivity of CP-506 toward hypoxia in vivo but could also be the result of different levels of hypoxia in the model. A study that investigates the relationship between adducts detected in areas of the tumor with different levels of hypoxia should be performed to ultimately answer this question. Nevertheless, here, we demonstrated that our approach can detect mono- and cross-linked adducts from CP-506 and its metabolites in DNA isolated from samples from in vivo studies.

In conclusion, we characterized the DNA adducts induced by CP-506 and its two metabolites in three models, which differed in complexity and biological significance. We identified different types of adducts (mono- and cross-linked adducts) derived from CP-506 or its metabolites. As these adducts are expected to exert different toxicities, they can be used in the future to monitor CP-506 efficacy and toxicity in patient samples collected during clinical trials to support the data on the susceptibility of patients to CP-506.

■ ASSOCIATED CONTENT

Supporting Information

The Supporting Information is available free of charge at https://pubs.acs.org/doi/10.1021/acs.chemrestox.1c00329.

Full details regarding the creation and strategy of using ^{15}N-labeled DNA for DNA adduct screening, cell cultures of tumor cell lines, DNA isolation, DNA quantitation by HPLC, and MS spectrum of m/z 666.3115 (PDF)

■ AUTHOR INFORMATION

Corresponding Author

Silvia Balbo − *Masonic Cancer Center and Division of Environmental Health Sciences, School of Public Health, University of Minnesota, Minneapolis, Minnesota 55455, United States;* orcid.org/0000-0002-7686-0504; Phone: 1-612-624-4240; Email: balbo006@umn.edu

Authors

Morwena J. Solivio − *Masonic Cancer Center, University of Minnesota, Minneapolis, Minnesota 55455, United States;* Present Address: Laboratory of Cellular and Molecular Immunology, VIB-Vrije Universiteit Brussel, Brussels, Belgium

Alessia Stornetta − *Masonic Cancer Center, University of Minnesota, Minneapolis, Minnesota 55455, United States*

Julie Gilissen − *Convert Pharmaceuticals SA, Liège 4000, Belgium*

Peter W. Villalta − *Masonic Cancer Center and Department of Medicinal Chemistry, University of Minnesota, Minneapolis, Minnesota 55455, United States;* orcid.org/0000-0002-0067-3083

Sofie Deschoemaeker − *Convert Pharmaceuticals SA, Liège 4000, Belgium;* Present Address: University of Minnesota Medical School, Minneapolis, MN, USA.

Arne Heyerick − *Convert Pharmaceuticals SA, Liège 4000, Belgium*

Ludwig Dubois − *Convert Pharmaceuticals SA, Liège 4000, Belgium; The D-Lab and The M-Lab, Department of Precision Medicine, GROW—School for Oncology and Developmental Biology, Maastricht Comprehensive Cancer Centre, Maastricht University Medical Centre, Maastricht 6229 ER, The Netherlands*

Complete contact information is available at: https://pubs.acs.org/10.1021/acs.chemrestox.1c00329

Author Contributions

M.J.S. and A.S. contributed equally. The manuscript was written through contributions of all authors. All authors have given approval to the final version of the manuscript.

Funding

This work was funded by the generous support from Convert Pharmaceuticals SA, Liege Belgium.

Notes

The authors declare no competing financial interest.

■ ACKNOWLEDGMENTS

The authors would like to thank Jeff B. Smaill and Adam V. Patterson at the University of Auckland for providing the drug compounds used in this study. The authors would also like to thank Romel Dator and Alex Strom for assistance with the extraction of bacterial DNA from bacteria obtained from the Coli Genetic Stock Center at Yale. We are also very thankful to Jan Theys, Ludwig J. Dubois, and Philippe Lambin at Maastricht University for their support in the preparation of this manuscript.

■ ABBREVIATIONS

AGC, automatic gain control; AKR1C3, aldo-keto reductase 1C3; amu, anomic mass unit; CNL, constant neutral loss; CP-506H, hydroxylamine metabolite; CP-506M, amine metabolite; ctDNA, calf thymus DNA; Da, Dalton; DDA, data-dependent acquisition; EASY-IC, easy internal calibration; EIC, extracted ion chromatogram; HAP, hypoxia-activated prodrug; HCD, higher energy collisional dissociation; HRAM, high-resolution/accurate-mass; IC_{50}, half maximal inhibitory concentration; LC, liquid chromatography; min, minute(s); ms, milliseconds; MS, mass spectrometry; s, seconds; SPE, solid phase extraction

■ REFERENCES

(1) Rajski, S. R.; Williams, R. M. DNA cross-linking agents as antitumor drugs. *Chem. Rev.* **1998**, *98*, 2723−2796.

(2) Farmer, P. B. Metabolism and reactions of alkylating agents. *Pharmacol. Ther.* **1987**, *35*, 301−358.

(3) Hunter, F. W.; Wouters, B. G.; Wilson, W. R. Hypoxia-activated prodrugs: paths forward in the era of personalised medicine. *Br. J. Cancer* **2016**, *114*, 1071−1077.

(4) Brown, J. M.; Wilson, W. R. Exploiting tumour hypoxia in cancer treatment. *Nat. Rev. Cancer* **2004**, *4*, 437−447.

(5) Wilson, W. R.; Hay, M. P. Targeting hypoxia in cancer therapy. *Nat. Rev. Cancer* **2011**, *11*, 393−410.

(6) Peeters, S. G. J. A.; Zegers, C. M. L.; Biemans, R.; Lieuwes, N. G.; van Stiphout, R. G. P. M.; Yaromina, A.; Sun, J. D.; Hart, C. P.; Windhorst, A. D.; et al. TH-302 in combination with radiotherapy enhances the therapeutic outcome and is associated with pretreatment [18F]HX4 hypoxia PET imaging. *Clin. Cancer Res.* **2015**, *21*, 2984−2992.
(7) Spiegelberg, L.; van Hoof, S. J.; Biemans, R.; Lieuwes, N. G.; Marcus, D.; Niemans, R.; Theys, J.; Yaromina, A.; Lambin, P.; et al. Evofosfamide sensitizes esophageal carcinomas to radiation without increasing normal tissue toxicity. *Radiother. Oncol.* **2019**, *141*, 247−255.
(8) Spiegelberg, L.; Houben, R.; Niemans, R.; de Ruysscher, D.; Yaromina, A.; Theys, J.; Guise, C. P.; Smaill, J. B.; Patterson, A. V.; et al. Hypoxia-activated prodrugs and (lack of) clinical progress: The need for hypoxia-based biomarker patient selection in phase III clinical trials. *Clin. Transl. Radiat. Oncol.* **2019**, *15*, 62−69.
(9) Patterson, A. V.; Ferry, D. M.; Edmunds, S. J.; Gu, Y.; Singleton, R. S.; Patel, K.; Pullen, S. M.; Hicks, K. O.; Syddall, S. P.; et al. Mechanism of action and preclinical antitumor activity of the novel hypoxia-activated DNA cross-linking agent PR-104. *Clin. Cancer Res.* **2007**, *13*, 3922−3932.
(10) Houghton, P. J.; Lock, R.; Carol, H.; Morton, C. L.; Phelps, D.; Gorlick, R.; Kolb, E. A.; Keir, S. T.; Reynolds, C. P.; et al. Initial testing of the hypoxia-activated prodrug PR-104 by the pediatric preclinical testing program. *Pediatr. Blood Cancer* **2011**, *57*, 443−453.
(11) Konopleva, M.; Thall, P. F.; Yi, C. A.; Borthakur, G.; Coveler, A.; Bueso-Ramos, C.; Benito, J.; Konoplev, S.; Gu, Y.; et al. Phase I/II study of the hypoxia-activated prodrug PR104 in refractory/relapsed acute myeloid leukemia and acute lymphoblastic leukemia. *Haematologica* **2015**, *100*, 927−934.
(12) Guise, C. P.; Abbattista, M. R.; Singleton, R. S.; Holford, S. D.; Connolly, J.; Dachs, G. U.; Fox, S. B.; Pollock, R.; Harvey, J.; et al. The bioreductive prodrug PR-104A is activated under aerobic conditions by human aldo-keto reductase 1C3. *Cancer Res.* **2010**, *70*, 1573−1584.
(13) Stornetta, A.; Villalta, P. W.; Hecht, S. S.; Sturla, S. J.; Balbo, S. Screening for DNA alkylation mono and cross-linked adducts with a comprehensive LC-MS(3) adductomic approach. *Anal. Chem.* **2015**, *87*, 11706−11713.
(14) Balbo, S.; Hecht, S. S.; Upadhyaya, P.; Villalta, P. W. Application of a high-resolution mass-spectrometry-based DNA adductomics approach for identification of DNA adducts in complex mixtures. *Anal. Chem.* **2014**, *86*, 1744−1752.
(15) Stornetta, A.; Villalta, P. W.; Gossner, F.; Wilson, W. R.; Balbo, S.; Sturla, S. J. DNA adduct profiles predict *in vitro* cell viability after treatment with the experimental anticancer prodrug PR104A. *Chem. Res. Toxicol.* **2017**, *30*, 830−839.
(16) Stornetta, A.; Deng, K.-C. K.; Danielli, S.; Liyanage, H. D. S.; Sturla, S. J.; Wilson, W. R.; Gu, Y. Drug-DNA adducts as biomarkers for metabolic activation of the nitro-aromatic nitrogen mustard prodrug PR-104A. *Biochem. Pharmacol.* **2018**, *154*, 64−74.
(17) van der Wiel, A. M. A.; Jackson-Patel, V.; Niemans, R.; Yaromina, A.; Lui, E.; Marcus, D.; Mowday, A. M.; Lieuwes, N. G.; Biemans, R.; et al. Selectively targeting tumor hypoxia by CP-506, a next-generation hypoxia-activated prodrug. Manuscript submitted.
(18) Frank, R.; Hargreaves, R. Clinical biomarkers in drug discovery and development. *Nat. Rev. Drug Discovery* **2003**, *2*, 566−580.
(19) Stornetta, A.; Zimmermann, M.; Cimino, G. D.; Henderson, P. T.; Sturla, S. J. DNA adducts from anticancer drugs as candidate predictive markers for precision medicine. *Chem. Res. Toxicol.* **2017**, *30*, 388−409.

https://doi.org/10.1021/acs.chemrestox.1c00329
Chem. Res. Toxicol. 2022, 35, 275−282